ChemComm

Few-layer black phosphorus nanoparticles

Journal:	*ChemComm*
Manuscript ID	CC-COM-11-2015-009150.R1
Article Type:	Communication
Date Submitted by the Author:	30-Nov-2015
Complete List of Authors:	Sofer, Zdenek; Institute of Chemical Technology, Prague, Department of Inorganic Chemistry Bouša, Daniel; Institute of Chemical Technology, Department of Inorganic Chemistry Luxa, Jan; Institute of Chemical Technology Prague, Department of Inorganic Chemistry Mazanek, Vlastimil; Institute of Chemical Technology, Prague, Department of Inorganic Chemistry Pumera, Martin; Nanyang Technological University, Chemistry and Biological Chemistry

Chemical Communications

Communication

Few-layer black phosphorus nanoparticles

Zdenek Sofer*[a], Daniel Bouša[a], Jan Luxa[a], Vlastimil Mazanek[a], and Martin Pumera*[b]

Received 00th January 20xx,
Accepted 00th January 20xx

DOI: 10.1039/x0xx00000x

www.rsc.org/

Black phosphorus quantum dots and nanoparticles of a few layer thickness were prepared here and characterized by STEM, AFM, dynamic light scattering, X-ray photoelectron spectroscopy, X-ray diffraction, Raman spectroscopy and photoluminescence. Impact electrochemistry of the induvidual black phosphorus nanoparticles allows their size determination. The centrifugation of colloidal black phosphorus nanoparticles allowed separation of quantum dots with size up to 15 nm. These black phosphorus nanoparticles exhibit large band gap and are expected to find wide range of applications from semiconductors to biomolecule tags. The use of black phosphorus nanoparticles for vapour sensing was sucesfully demostrated.

Black phosphorus (BP) is member of family of layered materials and it received huge amount of interest in the past two years. While there is significant interest in layered transition metal dichalcogenides (such as MoS_2, WS_2 and others, which are binary compounds), the black phosphorus is material consisting from one element, similarly to graphite. Graphite can be exfoliated to single layer graphene[1], black phosphorus can be exfoliated to single layer, in this case of two atom thickness (refer to **Figure 1** for structure of black phosphorus). Such black phosphorus sheet is termed "phosphorene"[2] or "phosphane".[3] Black phosphorus has very interesting semiconducting and mechanical properties and it has been demonstrated that it can be employed in field-effect transistors.[4] In addition, it exhibits low toxicity.[5] Recently, synthesis of black phosphorus quantum dots by ultrasonication was reported. [6]

Graphene and layered transition metal dichalcogenides can be prepared in the form of nanometer size particles, so called quantum dots.[7, 8] Small dimensions bring additional quality to these layered materials. Since the research on black phosphorus is in its beginning, knowledge of properties of black phosphorus nanoparticles and quantum dots is limited. Here, we present facile preparation of black phosphorus nanoparticles and quantum dots and we investigate their optical and electronic properties.

Layered black phosphorus was prepared by previously reported procedures in quartz glass ampoule using Au/Sn alloy as solvent, red phosphorus and SnI_4 as a mineralizing agent.[9] Synthesized crystals of black phosphorus were milled using agate mortar and ultrasonicated in solvent used for subsequent milling for 30 minutes. Subsequently black phosphorus suspension in solvent was milled using Ultra Turrax disperser for different times and speeds in various solvents (**see Figure S1**). Systematic measurement of particle size dependences were performed for various milling speeds using dimethylformamide (DMF), 1-methyl-2-pyrolidone (NMP), bis(2-methoxyethyl) ether (DIGLYM) and acetonitrile (AN). The milling time was prolonged up to 6 hours. The black phosphorus nanoparticles were separated by centrifugation. For more experimental details see supporting information. The size and morphology of black phosphorus nanoparticles were investigated using AFM and STEM microscopy and dynamic light scattering (DLS). The STEM images of black phosphorus nanoparticles are shown in **Figure 2**. The observation showed irregular particles with size of about 20-100 nm (**Figure 2A**), however also larger particles with size of up to about 200 nm can be seen on samples before centrifugation (**Figure S2**). In addition the morphology was further investigated using AFM. The results of AFM microscopy together with height profiles

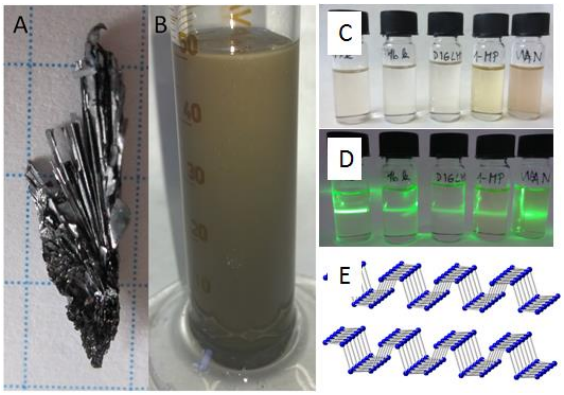

Figure 1. The optical image of black phosphorus crystal used for "top-down" synthesis of BP quantum dots (A) and colloidal solution of BP in DMF after 24 hours (B). The solution of black phosphorus quantum dots after centrifugation (C and D) and the structure of BP (E).

[a] Department of Inorganic Chemistry, University of Chemistry and Technology Prague, 166 28 Prague 6, Czech Republic. E-mail: zdenek.sofer@vscht.cz
[b] Division of Chemistry & Biological Chemistry, School of Physical and Mathematical Sciences, Nanyang Technological University, Singapore, 637371, Singapore. E-mail:pumera@ntu.edu.sg; Fax: +65 6791-1961

† Electronic Supplementary Information (ESI) available: Experimental section.

are shown in **Figure 2B**. The height profiles showed the platelet particles with lateral sizes of about 100 nm and height in the range of 2 – 5 nm (**Figure 2C** and **2D**) which corresponds to 3 to 10 layers of black phosphorus. Additional AFM images are shown in SI (**Figure S3**).

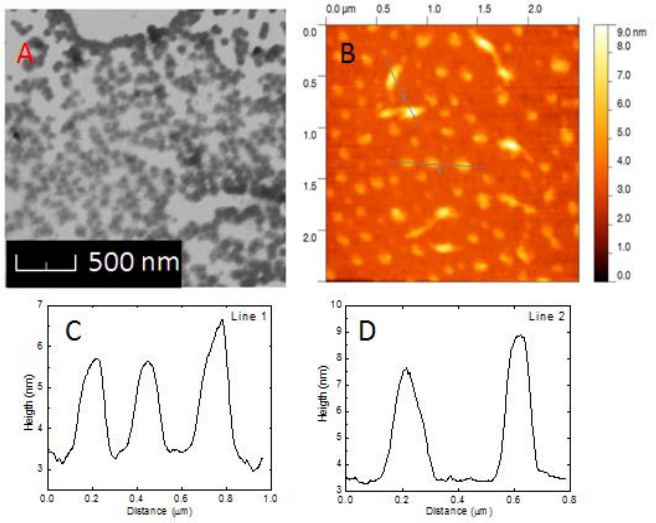

Figure 2. The STEM image of black phosphorus nanoparticles (**Figure 2A**). The scale bar corresponds to 500 nm. The AFM image of black phosphorus nanoparticles (**Figure 2B**) with corresponding line scans (**Figure 2C** and **Figure 2D**).

Even though the microscopy methods can give the information about particle size and morphology, only small proportion of particles can be investigated by such localized techniques. In order to obtain general information about particle size distribution we performed dynamic light scattering measurement. The first set of measurement was performed on milled BP after 48 hours of sedimentation. The images of BP colloids are shown in SI (**Figure S4**). The average size of such colloidal particles was in the range of 80 – 200 nm depending on the milling speed, time and solvent used. The yield of the milling procedure is strongly dependent on the solvent used reaching 33 wt.% for DIGLYM, 36 wt.% for DMF, 47 wt.% for NMP and 66 wt.% for AN. For the detail particle size distribution see supporting information (**Figure S5**). Acetonitrile gives the highest yield of BP nanoparticles, however the long term stability of such colloid is limited. The BP nanoparticles can be separated from the acetonitrile and transferred to DMF forming stable colloidal solution (**Figure S6**). Black phosphorus nanoparticles were separated from colloidal solution by centrifugation. The centrifugation was performed at 5000 and 10 000 rpm in order to further remove the larger particles and improve the particle size distribution. The results are shown in **Figure 4**. The measurement showed significant differences in the particle size and its distribution. In general, the largest particles are obtained for DMF using 11 000 rpm milling speed. The smallest BP nanoparticles, which had the size corresponding to quantum dots, are obtained for NMP and DMF at 5000 rpm centrifugation speed and at 10 000 rpm centrifugation speed smallest quantum dots are obtained in AN and DMF, respectively. The particle size distribution show the minimal size of about 15 nm and reaching maxima for 20-30 nm. The small BP quantum dots can be also separated by sedimentation (**Figure S7**). The broadening towards large particle diameter originates from platelet nanoparticle morphology as was shown by STEM and AFM. DLS on the other hand gives the information about average particle hydrodynamic radius which can be influenced by particle morphology.

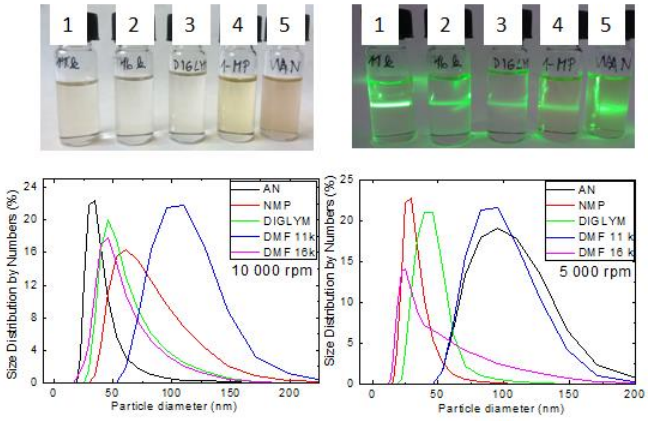

Figure 4. The particle size distribution measured by DLS for 5 000 rpm and 10 000 centrifugation speed. Upper image show the colloidal suspension of BP nanoparticles in different solvent and after irradiation with 532 nm laser. 1 – DMF, 11 000 rpm; 2 – DMF, 16 000 rpm, 3 – DIGLYM, 16 000 rpm; 4 – NMP, 16 000 rpm; 5 – AN, 16 000 rpm.

The impact electrochemistry method was investigated for measurement of particle size using inherent oxidation method.[10, 11] The measurement was performed at +1.0 V *vs*. Ag/AgCl in order to oxidize the black phosphorus to P^{5+} (for cyclic voltammograms see **Figure S8**).[10] The detail chronoamperograms show individual spikes originating from the oxidation of black phosphorus particles on the electrode surface. The charge passed during the particle interaction with the electrode surface corresponds to the particle size. Using the cube-like model for the particle, its size L can be evaluated using an equation (Eq. 1) corresponding to the Faraday's law:

$$L = \sqrt[3]{\frac{QM_r}{\rho Fz}} \qquad \text{(Eq. 1)}$$

where Q is the amount of net charge passing through during a collision (denoted by the area under the spike recorded in the chronoamperograms minus the average background signal) and M_r is the relative molecular mass of the phosphorus (30.974 g/mol). ρ is the density of the black phosphorus (2.69 g/cm^3), F is Faraday's constant (96485 C/mol), and z is the number of electrons transferred during phosphorus oxidation

(5 electorns). The detail chronoamperograms for the samples prepared by milling at 16 000 rpm in DMF for 0.5 hours and 6 hours, respectively are shown in **Figure 5**. The smallest spikes which can be detected with the current noise presented in obtained data indicate the minimal particle size of about 150 – 200 nm (**Figure 5B** and **Figure 5D**). The longer record of chronoamperograms between the samples milled for 0.5 hour and 6 hours (**Figure 5A** and **Figure 5C**) show significant reduction of large spike concentration indicating only minimal concentration of large particles after longer milling period. The individual small spikes in **Figure 5D** correspond to the cube-like particles with edge lenght in the range of 350 - 450 nm which is close to detection limit of demonstrated method. This indicates high concentration of small radius particles. For the detailed calculation of particle size for various samples see supporting Information (**Figure S9** and **Figure S10**).

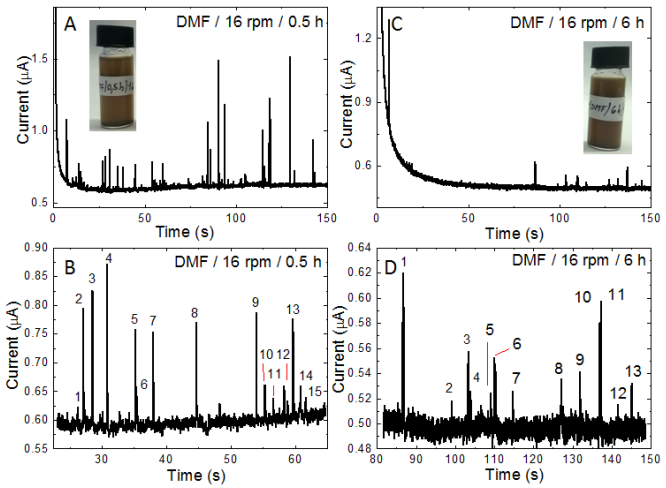

Figure 5. The chronoamperograms of black phosphorus milled at 16 000 rpm for 0.5 hour (**Figure 5A**) and 6 hours (**Figure 5C**) and the corresponding enlarged chronoamperograms (**Figure 5B** for 0.5 hour milling and **Figure 5D** for 6 hours milling).

The chemical analysis using XPS was performed to investigate the chemical composition of black phosphorus nanoparticles. The survey spectrum and high resolution spectrum of P 2p peak are shown in **Figure 6A** and **Figure 6B**. Significant twining of black phosphorus 2p peak originates from surface oxidation. The first peak with maxima at 129.9 eV originates form black phosphorus and the second maxima at 134.4 eV can be attributed to the surface oxidation and presence of P^{5+} in the form of phosphoric acid formed on the surface of black phosphorus.[3] The surface oxidation of black phosphorus was reported by several authors.[12, 13] In our case it can be caused by drying of black phosphorus nanoparticles solution on the surface of gold coated silicon wafer used for XPS measurement.

Further structural measurements were performed using Raman spectroscopy. The Raman spectra consist of three phonon modes donates as A^1_g, B_{2g} and A^2_g.[14] In bulk black

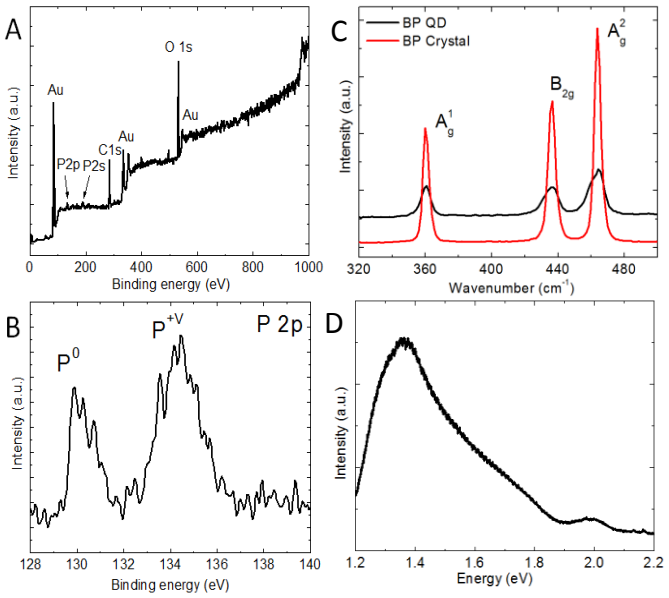

Figure 6. The XPS survey spectrum of black phosphorus nanoparticles (**Figure 6A**) and the detail spectra of P 2p (**Figure 6B**). The Raman spectra (**Figure 6C**) of black phosphorus nanoparticles and bulk crystal. The photoluminescence spectra (**Figure 6D**) of phosphorus nanoparticles.

phosphorus crystal these phonon modes are located at 362.1 cm^{-1}, 438.5 cm^{-1} and 465.6 cm^{-1} for A^1_g, B_{2g} and A^2_g which is in good agreement with the values reported in literature.[15] The reduction in number of layer is not accompanied by significant shift in phonon modes wavenumbers. However the broadening of A^1_g, B_{2g} and A^2_g phonon modes was previously observed together with intensity reduction.[16] The Raman spectra of bulk black phosphorus and exfoliated black phosphorus nanoparticles are shown in **Figure 6C**. We can observe significant broadening of A^1_g and B_{2g} phonon modes after exfoliation. For the A^1_g mode the broadening was 2.1 cm^{-1}, while for the B_{2g} the observed broadening associated with the formation of black phosphorus nanoparticles was 4.8 cm^{-1}. In addition we can observe significant changes in the shape and also the position of A^2_g phonon mode. We can observe the shift of 1 cm^{-1} towards higher wavenumbers and also twining of this phonon mode in comparison with bulk crystal. The second maximum is located at about 459.6 cm^{-1}. Such shape of A^2_g phonon mode is associated to the double layer of black phosphorus. This is in good agreement with AFM measurement which showed particles with height corresponding to 2 – 10 layers of black phosphorus. The photoluminescence spectra (**Figure 6D**) show broad luminescence band with maximum at 1.36 eV (912 nm). This corresponds to the double layer of black phosphorus.[17, 18] The maximum is slightly shifted towards higher energy compared

to reported values (1.29 eV). This can be associated with the oxidation of black phosphorus surface, which was also documented by XPS measurement. The structure of black phosphorus nanoparticles was further characterized by X-ray diffraction. The weak reflections originating from (0k0) reflections were observed. The broadening of (020) reflection corresponds to crystallite size of about 50 nm calculated according to Scherrer formula. The X-ray diffractogram is shown in **Figure 7**, left pannel.

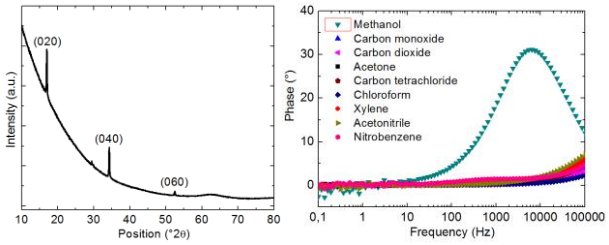

Figure 7. Left: The X-ray diffractogram of black phosphorus nanoparticles. Right: The Impedance phase spectra of black phosphorus nanoparticles using various vapors of solvents and gases.

The possible further applications of black phosphorus nanoparticles towards gas sensing were investigated using impedance spectroscopy and black phosphorus nanoparticles modified interdigitated electrode (**Figure 7**, right pannel). The dry air saturated with solvent vapor at 20 °C was used for testing in all cases. Such simple sensor shows the detection capabilities of black phosphorus nanoparticles towards highly toxic methanol. The results indicate that the detection abilities are related to the magnitude of dielectric constant (methanol 32.7) and also chemical composition, since the nitrobenzene has the value of dielectric constant close to that of methanol. We also tested the detection limit of methanol vapor, with results shown in **Figure S11**. The results indicate that the limit of detection is slightly below 2500 ppm (V/V) of methanol vapor, with clearly visible phase peak at around 4 kHz. The limit of methanol vapour concentration immediately dangerous to the life or healt is 6000 ppm according to The National Institute for Occupational Safety and Health.[19] The presence of hydroxyls functional group will probably play important role in interaction with black phosphorus surface influencing its impedance at different frequencies.

In summary, we have developed method for preparation of few layer thin black phosphorus nanoparticles which exhibit large band gap, much higher than the bulk black phosphorus. The influence of time and milling speed was systematically investigated for different solvents. The nanoparticles form highly stable colloidal suspensions in DMF and NMP. The impact electrochemistry method was utilized for the characterization of black phosphorus nanoparticles with detectable dimension below 200 nm. The yield of milling procedure over 60 wt.% was obtained for nanoparticles with size of about 100 nm. The colloidal solution of black phosphorus quantum dots with dimensions up to 15 nm can be obtained by centrifugation and also by sedimentation. The application of black phosphorus nanoparticles for gas sensing using impedimetric measurement was demonstrated with good sensitivity towards water and methanol. These black phosphorus nanoparticles shall find applications in wide areas of research, from biocompatible biomolecules tags to semiconductor devices.

Acknowledgements

M.P. acknowledges a Tier 2 grant (MOE2013-T2-1-056; ARC 35/13) from the Ministry of Education, Singapore. Czech side research was supported by Czech Science Foundation (GACR No. 15-09001S) and by Specific university research (MSMT No. 20/2015).

Notes and references

1. E. Fitzer, K.-H. Kochling, H. Boehm and H. Marsh, *Pure Appl. Chem.*, 1995, **67**, 473-506.
2. H. Liu, A. T. Neal, Z. Zhu, Z. Luo, X. Xu, D. Tománek and P. D. Ye, *ACS Nano*, 2014, **8**, 4033-4041.
3. A. Favron, E. Gaufrès, F. Fossard, A.-L. Phaneuf-L'Heureux, N. Y. Tang, P. L. Lévesque, A. Loiseau, R. Leonelli, S. Francoeur and R. Martel, *Nature Materials*, 2015.
4. J. Kang, J. D. Wood, S. A. Wells, J.-H. Lee, X. Liu, K.-S. Chen and M. C. Hersam, *ACS Nano*, 2015, **9**, 3596-3604.
5. N. M. Latiff, W. Z. Teo, Z. Sofer, A. C. Fisher and M. Pumera, *Chem. Eur. J.*, 2015, **21**, 13991-13995.
6. X. Zhang, H. Xie, Z. Liu, C. Tan, Z. Luo, H. Li, J. Lin, L. Sun, W. Chen and Z. Xu, *Angew. Chem. Int. Ed.*, 2015, **54**, 3653-3657.
7. M. Bacon, S. J. Bradley and T. Nann, *Particle & Particle Systems Charact.*, 2014, **31**, 415-428.
8. D. Gopalakrishnan, D. Damien, B. Li, H. Gullappalli, V. K. Pillai, P. M. Ajayan and M. M. Shaijumon, *Chem. Commun.*, 2015, **51**, 6293-6296.
9. L. Wang, Z. Sofer and M. Pumera, *ChemElectroChem*, 2015, **2**, 324-327.
10. W. Cheng and R. G. Compton, *TrAC, Trends Anal. Chem.*, 2014, **58**, 79-89.
11. M. Pumera, *ACS Nano*, 2014, **8**, 7555-7558.
12. M. Edmonds, A. Tadich, A. Carvalho, A. Ziletti, K. O'Donnell, S. Koenig, D. Coker, B. Özyilmaz, A. C. Neto and M. Fuhrer, *ACS applied materials & interfaces*, 2015, **7**, 14557-14562.
13. J. D. Wood, S. A. Wells, D. Jariwala, K.-S. Chen, E. Cho, V. K. Sangwan, X. Liu, L. J. Lauhon, T. J. Marks and M. C. Hersam, *Nano Lett.*, 2014, **14**, 6964-6970.
14. A. Castellanos-Gomez, L. Vicarelli, E. Prada, J. O. Island, K. Narasimha-Acharya, S. I. Blanter, D. J. Groenendijk, M. Buscema, G. A. Steele and J. Alvarez, *2D Materials*, 2014, **1**, 025001.
15. S. Sugai and I. Shirotani, *Solid State Commun.*, 1985, **53**, 753-755.
16. W. Lu, H. Nan, J. Hong, Y. Chen, C. Zhu, Z. Liang, X. Ma, Z. Ni, C. Jin and Z. Zhang, *Nano Research*, 2014, **7**, 853-859.
17. J. Yang, R. Xu, J. Pei, Y. W. Myint, F. Wang, Z. Wang, S. Zhang, Z. Yu and Y. Lu, *arXiv preprint arXiv:1504.06386*, 2015.
18. S. Zhang, J. Yang, R. Xu, F. Wang, W. Li, M. Ghufran, Y.-W. Zhang, Z. Yu, G. Zhang and Q. Qin, *ACS Nano*, 2014, **8**, 9590-9596.
19. http://www.cdc.gov/niosh/idlh/67561.html